11th. World Congress on Computational Mechanics (WCCM XI)
5th. European Conference on Computational Mechanics (ECCM V)
6th. European Conference on Computational Fluid Dynamics (ECFD VI)
July 20 - 25, 2014, Barcelona, Spain

NON-HOMOGENEOUS LOCALIZED KELVIN-VOIGT MODEL FOR ESTIMATION OF DYNAMICAL BEHAVIOUR OF STRUCTURES WITH BOLTED JOINTS

Anuj Sharma[1*], Wolfgang Mueller-Hirsch[1], Sven Herold[2] and Tobias Melz[2]

[1] Division Automotive Electronics, AE/EDE3, Robert Bosch GmbH, Robert-Bosch-Strasse 2, Schwieberdingen, 71701 Germany,
anuj.sharma2@de.bosch.com,wolfgang.mueller-hirsch@de.bosch.com
[2] Division Smart Structures, Fraunhofer Institute for Structural Durability and System Reliability LBF, Bartning Strasse 47, 64289 Darmstadt, Germany,
sven.herold@lbf.fraunhofer.de, melz@szm.tu-darmstadt.de

Key words: *Strcutural Vibrations, Contact Problems, Joint Stiffness, Structural Damping*

Structures with contact interfaces show a non-linear behaviour with predominance of local energy dissipation in comparison to inherent material damping losses. This paper implements an equivalent local discrete spring-damper system at the contact interface based on generalized Hertz and Mindlin contact models for the definition of contact stiffness, with the motivation of capturing the major non-linear effects of predominant structural modes. In contrast to many time domain methods, the present model is implemented in the frequency domain to enable advantages of easy modelling and reduced computational time for various practical applications. A double layered beam with four bolted joints is used as base model for test and validation of the contact model. A pressure dependent joint model is illustrated in this paper to obtain the equivalent contact stiffness in normal and tangential directions. For excitations provoking tangential relative motion, the region of micro slip existing between the stick and sliding region is idealized for maximum damping. The structure's dynamic behaviour is quantitatively studied for a variation of bolt pretension (variation in contact pressure). A quantitative model verification and parameter study of the base model has been done with a set of experiments. Results have shown a good match for both eigenfrequency and modal damping between simulation and experiment. It can be concluded for the present contact model, that the model shows good convergence with experimental investigations and thus can be used for lightly damped non-linear systems at very efficient computational times.

List of Symbols

δ_N	Normal penetration
δ_T	Relative tangential displacement
δ_{N0}	Penetration at zero contact pressure
λ	Parameter for exponential contact law
ν	Poisson's ratio
$\Phi(z)$	Probablity density function of surface roughness
$\phi(z)$	Probablity distribution function of surface roughness
σ	Standard deviation of surface roughness
τ	Shear stress
τ_0	Maximum Shear stress
d	Local damping at contact interface
E	Elastic modulus
E^*	Equivalent mean elastic modulus in Hertz model
E^*	Radius of sphere
F_N	Normal contact force
F_T	Tangential contact stiffness
G	Shear modulus
G^*	Mean Shear modulus in Hertz model
k_N	Normal contact stiffness
k_T	Tangential contact stiffness
$P(r)$	Hertzian pressure distribution
P_0	Maximum pressure
P_N	Normal contact pressure
P_{mf}	Parameters governing P_m location
P_{N0}	Initial contact pressure at interface with no loading
Pm	Contact Pressure at the location of maximum dissipation
R^*	Equivalent mean radius of elastic spheres in Hertz model
r_c	Contact radius
u_z	Normal displacement of elastic half space

1 Introduction

Today's industrial products are extensively using different forms of joints and fasteners. The joints play a significant role in transferring loads and imparting damping to the assembled structure. To obtain a good operational accuracy of the products, the effect of joints has been studied in the past and still been studied on. With advent of high computing capabilities, the demand for a proper modelling and simulation of joints behaviour has increased. The numerical model can predict the real behaviour only with correct definitions of system stiffness and damping. Accurate definition and implementation of contact stiffness and damping has been a challenge for researchers and engineers. Contact stiffness is viewed to be defined through the contact pressure distribution and damping as function of dissipation occurring at the interface.
In literature, lot of analytical work can be found on various contact models and their respective parameters influencing the dynamical behaviour of structures. Work of Hertz has been one of the earliest in modelling contact of elastic half spaces. Further extensions were done by Mindlin (1949) [1] to tangential contact model. More detailed definition of contact model based on surface roughness is studied by Greenwood and Williamson (1966) [8]. The emphasis was laid on the determination of actual contact area and force using stochastic fit for the surface roughness of nominally flat surfaces. Experimental investigations too have been significant in determination of the pressure distribution from bolted joints. Gould and Mikic (1972)[3], Ziada and Abd (1980) [4] showed that the contact pressure is parabolic in nature with circular influence zone of 3.5 times diameter of bolt . Also, the pressure profile is independent of the bolt twisting moment. Nanda and Behera (2000) [9] empirically established that to obtain an uniform pressure distribution, the bolts have to be separated by an approximate distance of twice times diameter of connecting bolt.
To study the effects of contact non-linearity on the assembled structures undergoing dynamical excitations, a lot has been accomplished in both experimental and analytical-numerical modelling, in terms of estimation of the joint dissipation and analysing its impact on dynamical behaviour of structures. The damping in assembled structures is predominately from relative movement at the interface in comparison to the inherent material damping [7], [5], when no external damping treatment is applied. The relative motion is divided into two stages. When the complete surface moves relative to the other, is referred as gross or macro-slip. Before the gross slip is achieved, the low levels of excitation produce micro levels of relative movement in contact interface and are termed as micro-slip. Both the sources of dissipation have predominant effect on dynamical characteristics, wherein the complete macro slip results in failure of mating parts whereas only micro-slip or combination of macro-micro slip will significantly contributes to optimum damping [13]. An extensive study on dissipation-hysteresis curves of lap joints were experimentally studied by Gaul and Lenz [10]. A discrete frictional law - Valanis lumped model was implemented in same to match the results of experiments, to significantly capture effect of stick and slip [10]. Other models too are also present in plenty to capture the effect of non-linearities through contacts interfaces.
Although above mentioned models have been successful in depicting the complex be-

haviour of effect contacts, their implementation for large models involving millions of elements does not look to be practical. Harmonic Balance method and its derivative methods, have been advantageous for their implementation directly in the frequency domain. However, the frequency domain description again solves a non-linear equation and finds good acceptance for systems that experience periodicity. For real time excitation, like random excitation, both methods do not present an effective and practical solution. The demand is of a linear model that can be utilized for large models and simultaneously incorporate the effect of non-linear contact to predominant significant modes. This paper presents an approach to model contact interface with inhomogeneous Kelvin-Voigt elements, wherein the stiffness of element account for the contact stiffness and loss elements - dampers for contact damping. The spring stiffness is calculated based on the contact pressure distribution and contact damping is thought as a contribution from combination of three region undergoing no slip or stick, micro-slip and macro-slip. The dissipation in respective region is defined with on some stochastic distribution based on the contact pressure existing at the interface. To decide on the feasibility and limitations of the model, experimental validations are performed on an academic example of double layered beam with bolts. Two sets of experiments are performed with one studying the effect of contact pressure using experimental modal analysis and other the excitation amplitude using a shaker stinger experiment, on the eigenfrequency and modal damping of the base model.

2 Theoretical background - Normal and Tangential Contact

The normal contact between two rough surfaces can be modelled as the integration of various discrete point to point contacts in the interface region. The contact can be defined based on generalized Hertz contact model. The Hertzian pressure distribution [8] can be defined in contact interface with contact radius of r_c as,

$$P(r) = P_0\sqrt{\left(1 - \frac{r^2}{{r_c}^2}\right)}, \quad 0 \leq r \leq r_c \tag{1}$$

For a rigid sphere in contact with an elastic half space, the displacement u_z of the points on the surface of the contact interface can be expressed in terms of the normal penetration, radius of sphere and contact radius. The displacement u_z can also be equated to the resulting deformation from Hertzian pressure distribution (with no friction), as shown in below equation.

$$u_z = \delta_N - \frac{r^2}{2R} = \frac{\pi P_0 \left(2r_c^2 - r^2\right)\left(1 - \nu^2\right)}{4r_c E} \tag{2}$$

The above equations when extended for two elastic spheres in contact [8], [15],brings change in radius of spheres R and elastic constant E used in equation 2, with equivalent

radius R^* and equivalent elastic constant E^* of the combined spheres in contact expressed as,

$$\begin{aligned} \frac{1}{R^*} &= \frac{1}{R_1} + \frac{1}{R_2} \\ \frac{1}{E^*} &= \frac{1-\nu_1^2}{E_1} + \frac{1-\nu_2^2}{E_2} \end{aligned} \tag{3}$$

Substituting equation 3 into 2, the contact radius and the maximum pressure can be obtained as,

$$r_c^2 = \delta_N R^* \tag{4}$$

$$P_0 = \frac{2}{\pi} E^* \sqrt{\left(\frac{\delta_N}{R^*}\right)} \tag{5}$$

The normal force existing at the contact interface due to the Herztian pressure distribution is calculated by integrating the pressure distribution over the contact area. With the use of maximum pressure from equation 5, force is reduced to a function of the penetration and elastic constants.

$$F_N = \int_0^{r_c} P(r) 2\pi r dr = \frac{2}{3}\pi P_0 r_c^2 = \frac{4}{3} E^* {\delta_N}^{\frac{3}{2}} {R^*}^{\frac{1}{2}} \tag{6}$$

Estimation of the normal contact forces allows the definition of normal contact stiffness as the derivative of normal contact force with respect to the penetration. The normal contact stiffness is proportionally dependent on the contact radius and elastic constant. Hence for a given material properties, larger contact area will result in a higher stiffness.

$$k_N = \frac{dF_N}{d\delta_N} = 2E^* \sqrt{\delta_N R^*} = 2E^* r_c \tag{7}$$

Although the obtained normal contact stiffness is dependent on the contact interface dimensions (r_c), the idea of two elastic spheres in contact is used as a depiction of the single asperity contact [15] in macroscopic models, eliminating the dependence on contact radius variation locally. Each local contact pair is attributed with a spring stiffness joining the contact and target point, whose modelling with commercial software is discussed in section explaining the pressure dependent joint.

For loading in the tangential direction, friction plays the role in defining the state of slip or stick. Mindlin (1949) [1] extended the Hertz elastic normal contact for tangential

contacts, with a stress distribution $\tau(r)$ over the contact interface. Respectively, the tangential forces F_T and displacement δ_T for two spherical asperities in the contact are obtained [18],[15].

$$\tau(r) = \tau_0 \left(1 - \frac{r^2}{r_c^2}\right)^{-\frac{1}{2}} \tag{8}$$

$$F_T = \int_0^{r_c} \tau(r)\, 2\pi r dr = 2\pi\tau_0 r_c^2 \tag{9}$$

$$\delta_T = \frac{\pi\tau_0 r_c}{4G^*} \tag{10}$$

wherein, $\frac{1}{G^*} = \frac{2-\nu_1}{G_1} + \frac{2-\nu_2}{G_2}$.
Similar to the normal contact stiffness, the tangential stiffness can also be calculated as the derivative of the tangential contact force with respect to the tangential displacement, which is also dependent on the contact radius and equivalent mean shear modulus.

$$k_T = \frac{dF_T}{d\delta_T} = 8G^* r_c \tag{11}$$

The coupling between the normal and tangential contact stiffness can be calculated as a factor, depending only on the material properties of the contact interface materials and is independent of the contact geometry.

$$\frac{k_T}{k_N} = 4\frac{G^*}{E^*} \tag{12}$$

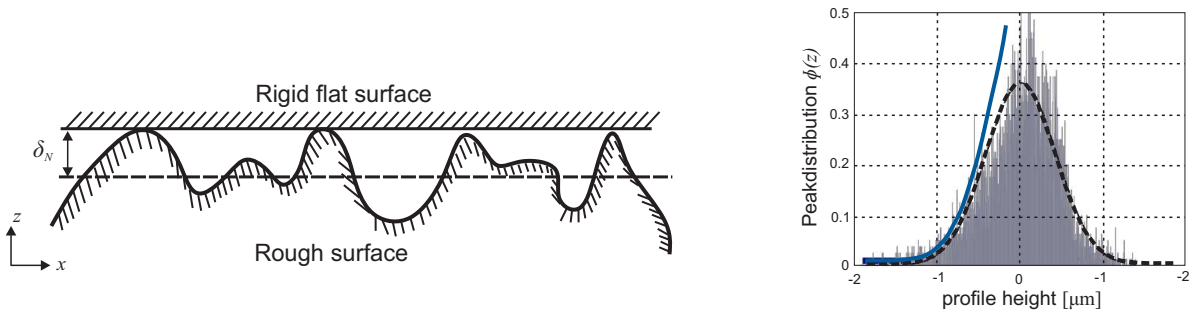

Figure 1: Contact between a rough surface and rigid plane. The normal gap or distance δ_N is calculated from a reference plane of rough surface. Height distribution of different peaks of rough surface with dashed lines showing a fit with Gauss-normal distribution. Solid blue line indicates the fit with an exponential distribution function

Greenwood and Williamson (1966) [2] developed a contact model based on the surface roughness. The peaks contributing for the initiation of contacts are characterized through the probability distribution and density function. Although a Gauss-Normal distribution can capture the variation of surface roughness quiet well, as shown in figure 1, analytical estimation of the number of contacts, area of contact and normal force is difficult. Here, an exponential distribution function is chosen, as it can be used easily to estimate the required variables analytically [14],[15]. Also, it sufficiently captures the influence from the peak locations than the other locations of the rough surface.

$$\phi(z) = \frac{e^{\left(-\frac{z}{\sigma}\right)}}{\sigma} \quad ; \quad \Phi(z) = e^{\left(-\frac{z}{\sigma}\right)} \tag{13}$$

Greenwood and Williamson (1966) surface based contact model is extended with the choice of exponential distribution of peaks in accordance to work of Willner (2004) [12], to define contact pressure based on the apparent contact area. The distribution function involving term of standard deviation σ, is used to define the normal contact parameter λ as the inverse of σ.

$$P_N = P_{N0}\ e^{\lambda(\delta_N - \delta_{N0})} \qquad \lambda = \frac{1}{\sigma} \tag{14}$$

The above expression defining the contact pressure consist of P_{N0}, which is taken as the initial contact pressure experienced for the two contacting surface placed over each other without loading. The initial penetration δ_{N0} at zero contact pressure can be estimated by extending the pressure-penetration curve backwards with an approximation of unit slope, as shown in figure 3. The next section will emphasize on using the pressure-penetration exponential relation for modelling the pressure dependent joint, to estimate the equivalent contact stiffness and damping based on variation in contact pressure distribution.

3 Pressure dependent joint - Contact Stiffness and Damping

As described in the previous section of defining a macroscopic asperity contact model based on the Herztian theory and surface roughness based model of Greenwood and Williamson, modelling of the contact interface as point to point contact at local discrete points is discussed in this section. A flat nominal surface has a large apparent contact with dispersed asperities and the forces on individual asperities will have no influence on the neighbour asperities [2]. Hence, a non-homogeneous independent definition of the contact stiffness and damping for each contact point pair (for individual asperity) can be formulated. A pressure dependent joint, as evident from its name, describes the local contact based on the contact pressure existing at the interface. With a change in the load steps, an update in the contact pressure and also the contact status leads to an equivalent change in the joint stiffness and damping.

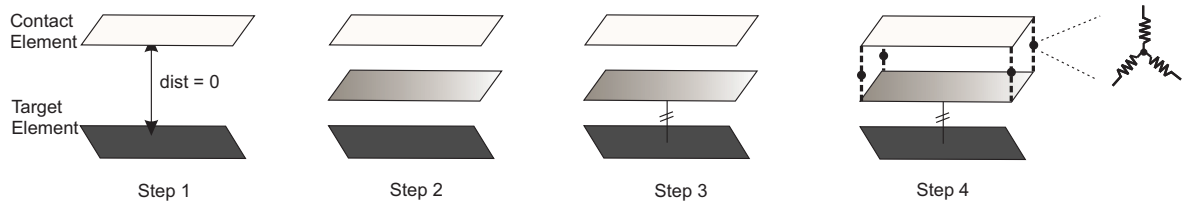

Figure 2: Steps in creation of pressure dependent joint between contact and target faces of assembled structure

Pressure Dependent Joint (PDJ) formation is a four step process, as depicted in figure 2. In the first step, the contact and target surface are discretized with regular finite elements. Complex and assembled geometry tend to have non-conforming meshes. To accommodate the effect of same, new target elements between the contact and old target elements are created in the second step. These target elements will be having the same orientation as the contact elements, resulting in a conformed mesh. In third step, a constraint equation between new and old target elements is created, enabling a fixed bonded contact between the two. In other words, the results of new target element nodes will be transferred directly to the old target element nodes. In the final step, three dimensional kelvin-voigt spring elements are inserted between the nodes of the contact and new target elements. ANSYS 14.5 has been used, wherein the surface to surface based contact defined from software is replaced with PDJ model.

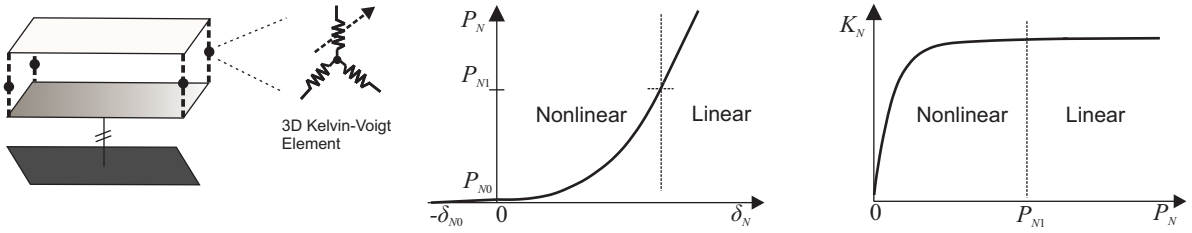

Figure 3: Unit cell of pressure dependent joint with non-linear normal contact stiffness governed by exponential pressure-penetration relation.

After the creation of conformed pressure dependent joint, definition of the spring stiffness is required for non-linear contact analysis. The exponential pressure-penetration relation as mentioned in equation 14, is used to calculate the normal stiffness density $K_N[\mathrm{N/mm^3}]$ by differentiating the pressure with respect to penetration [21]. For the exponential function, after a saturation limit, there will be very high increase in pressure values for a very small increment in penetration δ_N, which can cause difficulties in convergence. To overcome this problem, a linear extension of the curve is done with the same slope at the saturation point P_{N1}. The saturation point is chosen such that the stiffness variation with respect to pressure is stabilized and all predominant non-linear behaviour is covered before 75% of P_{N1}. Based on this, region before P_{N1} is considered non-linear and region after is linear, as shown in figure 3. The tangential stiffness are considered as linear and corresponding values of same are calculated based on updated values of the normal stiffness using equation 12. This assumption is valid for normal loading producing negligible relative displacement between the interfaces compared to the normal deformation.

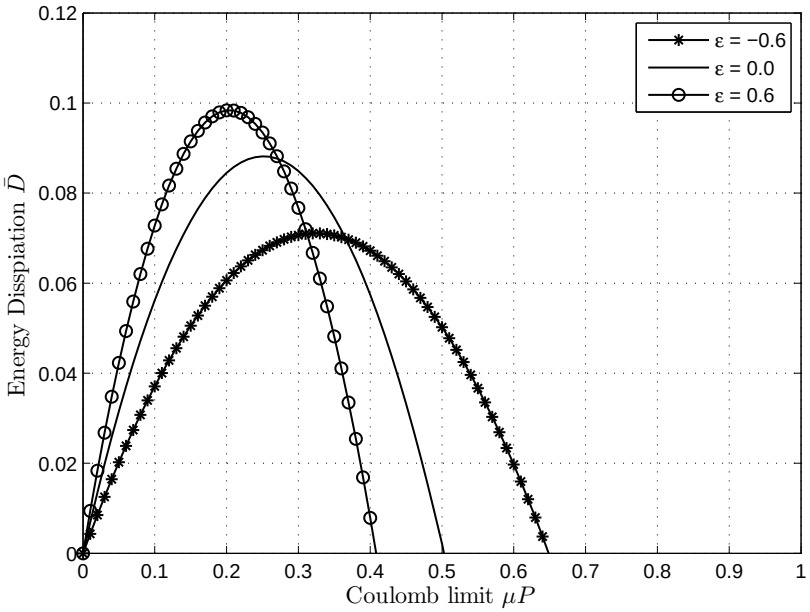

Figure 4: Non-dimensional dissipation plotted for variation in Coulomb friction limit over the contact interface [16]

For defining the contact damping, it is also proposed to have a localized definition of damping at the contact interface. The source of contact damping is the relative motion between the upper and lower parts of the jointed structure. Due to random distribution and height of asperities, the local relative displacement cannot be considered of same magnitude for each contact point pair. A generalization for a bolted joint can be done in terms of defining three zones, based on the relative displacement and Coulomb friction-limit. The region near bolt experiences hardly any relative displacement, with higher values of Coulomb friction and is referred as a region of stick. Region significantly away from the bolt will be experiencing substantial relative displacement with lower Coulomb friction and referred as gross slip or slide region. The region in between of stick and slip is regarded as micro-slip region, which experiences micro levels of relative displacement with moderate values of Coulomb friction. The micro slip region is assumed to carry more dissipation when compared to other two regions or at the boundary of two regions [6]. An example of clamped layered beam is studied by Damisa et al (2008) [16] to estimate the dissipation at interface in relation to non-uniform interface pressure. For a linear pressure variation $P(x) = P_0\left(1 + \frac{\varepsilon}{L}x\right)$ along the laminate interface length L, an analytical estimation of non-dimensional dissipation in relation to existing Coulomb friction limit is done. It can be deduced from results of Damisa et al (2008) [16], that the maximum dissipation exists at an intermediate pressure i.e. between the region having high and low contact pressure values, as shown in figure 4.

As damping is directly associated with the dissipation, similar local contribution from contact damping can be expected. Observed trend of dissipation can be modelled with combination of discrete damper elements, with local contribution based on a stochastic fit function having primary variable as contact pressure. This relates to defining the damping

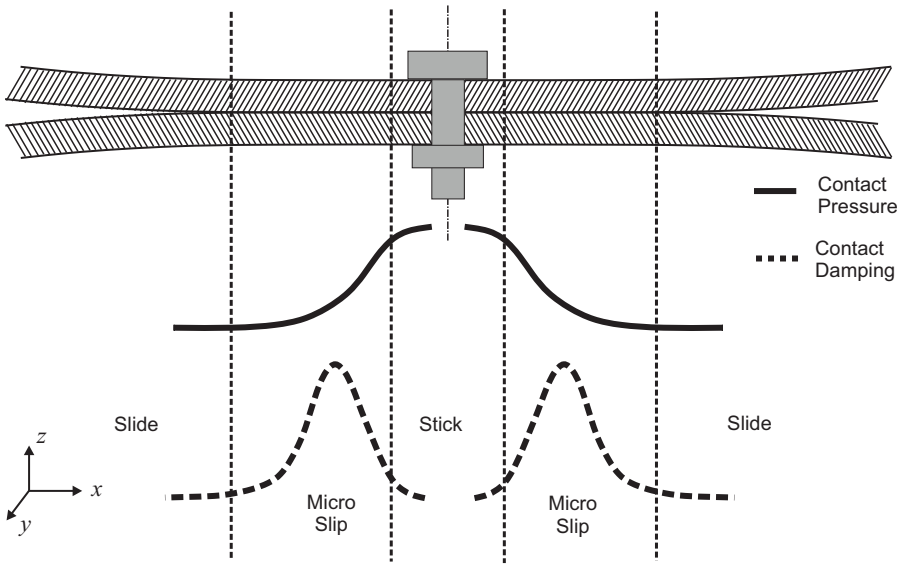

Figure 5: Division of regions in contact interface with pressure distribution obtained from bolt twisting moment and predicted damping distribution based on pressure distribution

with respect to only contact pressure, with an assumption of a constant friction coefficient and contact status. Static loading through bolt pretension with pressure dependent joint will provide the resultant contact pressure. Based on this pressure, a stochastic fit of the discrete damping distribution over the interface can be performed. A pictorial representation is shown in figure 5. This accommodates the effect of local dissipation occurring at the interface and the cumulative effect of same can be matched with the global estimation of damping from experiments.
To describe the local damping distribution, two sets of distributions from the conventional distribution functions are mentioned below.

Localized damping as an inverse absolute function of pressure distribution,

$$d(x,y) = \frac{d_{loc}}{|P(x,y) - P_m|} \tag{15}$$

Rayleigh damping distribution as a function of pressure distribution

$$d(x,y) = \left(\frac{P(x,y)}{P_m}\right) \exp\left(-\frac{1}{2}\left(\frac{P(x,y)}{P_m}\right)^2\right) \chi_r \tag{16}$$

where,

$$P_m = \frac{\max(P(x,y)) - \min(P(x,y))}{P_{mf}} \tag{17}$$

In above distributions, P_m refers to the corresponding pressure at a location, where the maximum dissipation is assumed to be occurring. χ_r is the scaling factor to control the

limits of damping value. P_m is evaluated based on equation 17, wherein P_{mf} is the parameter to locate the maximum dissipation position. P_{mf} is updated accordingly to match the results of experiments and is discussed in next section of experimental validation. The inverse absolute distribution is unbounded at $P(x, y) = P_m$ and requires more controlling parameters to predict a good approximation with the experimental values. The Normal, Log-normal, Weibull and other distributions could also be proposed, but due to increase in number of parameters (like standard deviation) in the formulation, they are avoided for now. The advantage with Rayleigh distribution is not only less parameters but also the distribution is predominately effective in micro-slip region. In this paper, the results are generated using Rayleigh damping distribution for defining the discrete local damping elements.
The definition of these distributions are modified to obtain a non-dimensional quantity, so as to accommodate the definition of local damping in terms of hysteretic elements or structural damping. The choice of visco-elastic damping elements is not advisable [20], as the global damping of combined structure from experiments results, as shown in tables 2,3 and 4, do not show a well defined dependence in relation to the frequency. Where as, the Structural damping is observed experimentally to have only influence from excitation amplitude and not based on frequency for harmonic loading. The next section will concentrate on validation of the proposed model with experimental observations.

4 Results and Comparisons

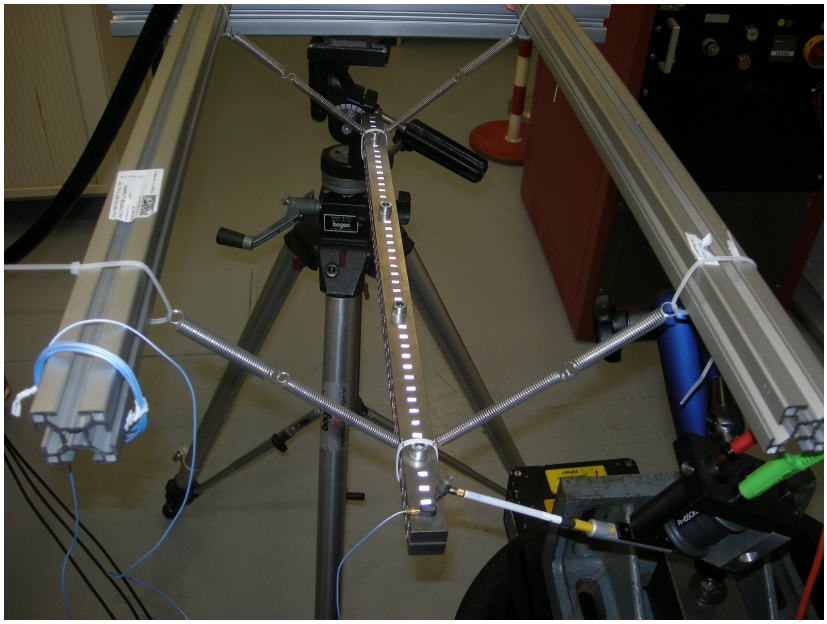

Figure 6: Experimental set-up of freely hanging base model for EMA with auto impulse hammer

The proposed contact model is tested using a base model of a double layered beam with 4 bolted joints. An individual beam has dimensions of 500mm x 20mm x 10mm and is

Table 1: EMA results of Eigenfrequency and modal damping ration for double layered beam with 4 bolted joints at different bolt pretensions

Mode	Eigenfrequency			Modal damping ratio		
	1Nm	3Nm	5Nm	1Nm	3Nm	5Nm
1	361.85	371.13	373.07	0.295	0.151	0.127
2	405.28	405.33	405.35	0.035	0.031	0.032
3	826.69	899.01	910.16	0.425	0.245	0.161
4	1106.17	1106.34	1106.42	0.026	0.025	0.026
5	1559.85	1720.03	1770.14	0.650	0.345	0.172
6	1738.85	1785.56	1808.14	0.095	0.173	0.092
7	1980.01	2080.21	2120.37	0.261	0.239	0.176
8	2145.97	2146.42	2146.52	0.031	0.028	0.027
9	2820.21	2980.15	3040.01	0.281	0.226	0.158

made of stainless steel, with four M6 size bolts used to connect two beams. Two sets of experiment are performed for the comparison with the simulation results. The first set of experiments will study the effect of the bolt load and the second set will concentrate on the effect of the excitation amplitude on the dynamical characteristics of the base model. In the first set of experiments, aim is to perform a quantitative study on distinctly the effect of the contact pressure (through the bolt twisting moment) on the eigenfrequency and modal damping of the base model. An Experimental Modal Analysis (EMA) with roving measurement of the base model is performed, using an auto controlled impulse hammer. The set-up is shown in figure 6. The auto controlled impulse hammer essentially excites the structure with same amplitude, for all measurement points. Hence, the effect of variation in excitation amplitude on modal parameters is eliminated. There are three sets of experiments performed with 1Nm, 3Nm and 5Nm bolt twisting moment. The choices are done to analyse the proposed contact model's capability to describe systems with non-linear (1Nm), moderately non-linear (3Nm) and slightly non-linear (5Nm) behaviour. The measured modal frequency and modal damping of the base model for different choices of the bolt twisting moment are shown in table 1.

Table 2: Comparison between EMA and PDJ simulation of base model having 1Nm bolt twisting moment with parameters $\lambda = 1400$ and $P_{mf} = 1.2$.

Mode	Eigenfrequency (Hz)			Modal damping ratio (%)		
	Exp.	Sim.	Error (%)	Exp.	Sim.	Error (%)
1	362	360	0.6	0.30	0.31	3.3
3	827	824	0.4	0.42	0.43	2.4
5	1560	1540	1.3	0.65	0.57	12.3
7	1980	2026	2.3	0.26	0.26	0.0
9	2820	2909	3.2	0.28	0.22	21.4

Looking at the experimental results, it can be observed that for modes 1,3,5,7 and 9 (highlighted in grey), there is a significant effect of the bolt load on both modal frequency and modal damping, whereas the rest of modes show very little effect of the bolt load.

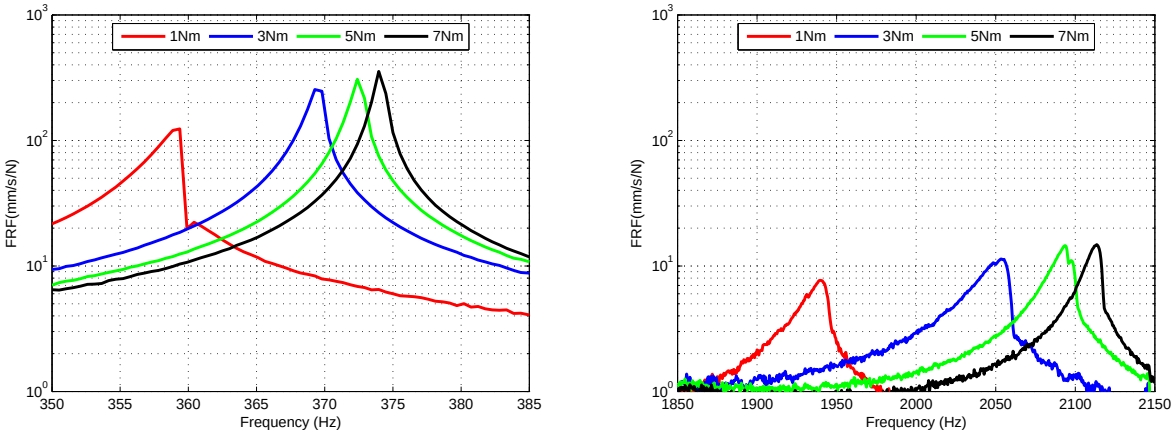

Figure 7: Effect of bolt load on shape of FRF (Frequency Response Function) mobility of base model observed in experimental modal analysis for mode 1 (left) and mode 7 (right)

This can be explained by looking at the mode shapes of corresponding modes. Modes 1,3,5,7 and 9 are the out-of-plane modes where as the rest are the in-plane modes. Firstly, the in-plane bending modes are hardly excited and if so also, they do not predominantly influence the contact interface. The individual beams ideally experiences the in-plane bending modes at same frequency and phase, experiencing very minimal effect of tangential coupling inducing relative motion between the two beams. Hence the effect from in plane bending modes are wholly accounted for material properties of the structure. Whereas for the out of plane bending or torsion modes, there is a proximity of the relative movement occurring between the top and lower beam. This is similar to phenomenon of beam bending theory, where the part of a beam above and below the neutral axis goes under compression and tension respectively. The contact interface can be thought as the neutral axis and relative motion at contact interface is accounted for the variation due to tension and compression. Hence, for the validation of proposed contact model, emphasis is paid on the out of plane bending modes for comparison with experimental results. The second observation on trends of both the eigenfrequency and modal damping are quiet obvious. With increase in the bolt twisting moment, the Eigen-frequency of structure also increases, as the contact stiffness is proportional to the contact pressure. Figure 7 shows the effect of bolt load on the symmetric shape of FRF. Similarly, the damping shows a reduction, as increase in bond pressure hinders the relative motion enabling decrease in the losses at contact interface. These observations confirm the choices of the bolt twisting moment of 1Nm, 3Nm and 5Nm as nonlinear, slightly nonlinear and linear behaviour respectively.

For simulation, the required elastic properties of steel are obtained by model updating of single beam with experiment modal analysis results. The elastic modulus E =196 GPa and poisson's ratio ν =0.3 are used. As the contact pair is between two identical materials i.e. $E_1 = E_2$, $\nu_1 = \nu_2$ and $G_1 = G_2$, the coupling factor as introduced in equation 12 can be calculated as

$$\frac{K_t}{K_n} = 2\frac{1-\nu}{2-\nu} = 0.83 \tag{18}$$

The contact parameter λ based on the definition of standard deviation of surface roughness, is chosen as a value of 2000 for initial calculations. The effect of this parameter is predominately on the eigenfrequency of the base model and is estimated with model updating for each case. The localized damping distribution parameter P_{mf} defining the location of maximum damping is chosen as 2 for initial calculation. The choice is a good guess with P_m as the mean of the maximum and minimum value of contact pressure. This parameter is varied after the best possible choice of λ. Modal damping is calculated as the ratio of damped strain energy to un-damped strain energy. A comparison of the eigenfrequency of experiment and simulation for each case of bolt twisting moment are given in table 2, 3 and 4 respectively.

Table 3: Comparison between EMA and PDJ simulation of base model having 3Nm bolt twisting moment with parameters $\lambda = 2100$ and $P_{mf} = 1.9$

Mode	Eigenfrequency (Hz)			Modal damping ratio (%)		
	Exp.	Sim.	Error (%)	Exp.	Sim.	Error (%)
1	371	372	0.3	0.15	0.16	6.7
3	899	883	1.8	0.25	0.26	4.0
5	1720	1721	0.1	0.35	0.34	2.9
7	2080	2130	2.4	0.24	0.23	4.2
9	2980	3028	1.6	0.23	0.22	4.3

Table 4: Comparison between EMA and PDJ simulation of base model having 5Nm bolt twisting moment with parameters $\lambda = 2150$ and $P_{mf} = 2$

Mode	Eigenfrequency (Hz)			Modal damping ratio (%)		
	Exp.	Sim.	Error (%)	Exp.	Sim.	Error (%)
1	373	374	0.3	0.13	0.12	7.7
3	910	890	2.2	0.16	0.15	6.3
5	1770	1743	1.5	0.17	0.21	23.5
7	2120	2148	1.3	0.18	0.15	16.7
9	3040	3050	0.3	0.16	0.15	6.3

The maximum error in the eigenfrequency for 1Nm bolt twisting moment is 3.3%, which is quiet a good match for a system experiencing strong non-linearity, as seen in figure 7. A very good estimation of modal damping ratio is also obtained with acceptable maximum error of 22%. For higher bolt twisting moment, the non-linearity from contacts is assumed to be less predominant in comparison to 1Nm load and hence the proposed contact model should also have a good convergence for the same.
Maximum eigenfrequency error of 2.4% and 2.2% are obtained for 3Nm and 5Nm bolt twisting case respectively, which are in acceptable range. The damping values show much more better convergence than in the case of 1Nm. The contact parameters (λ and P_{mf}) used for 3Nm and 5Nm cases were almost identical and hence the model can ideally be used for moderately and slightly non-linear system. It is interesting to look at the optimal choices of P_{mf} used for three cases of the bolt twisting moment. With increase in the

bolt twisting moment, the value of P_{mf} is also increasing and stabilizes with high bolt loads. This suggest that with increase in the contact pressure, the location of maximum dissipation also shifts. The variation in the modal damping ratio for 5Nm case is almost negligible for all modes in comparison to other two cases. This suggests that for higher bolt loads, the damping will stabilize for all modes and will coincide with definition of the structural damping, independent from frequency. Also, for all three cases of the bolt twisting moment, the simulation yielded negligible modal damping for in-plane modes. This fits the experimental observation discussed formerly about the negligible effect of the in-planes modes on dynamical characteristics of jointed structures, see table 1.

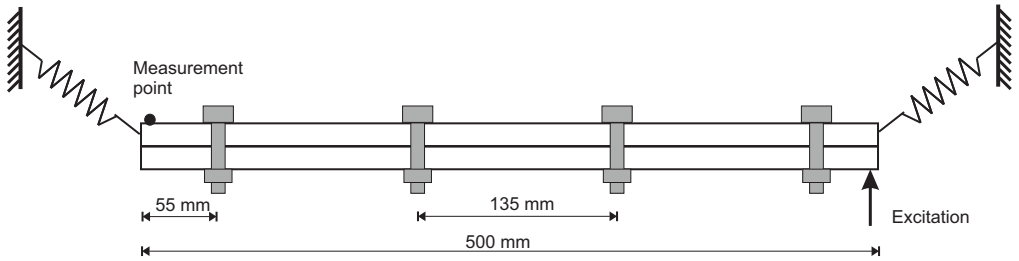

Figure 8: Shaker stinger experiment set-up of base model with excitation at right end and measurement at other end

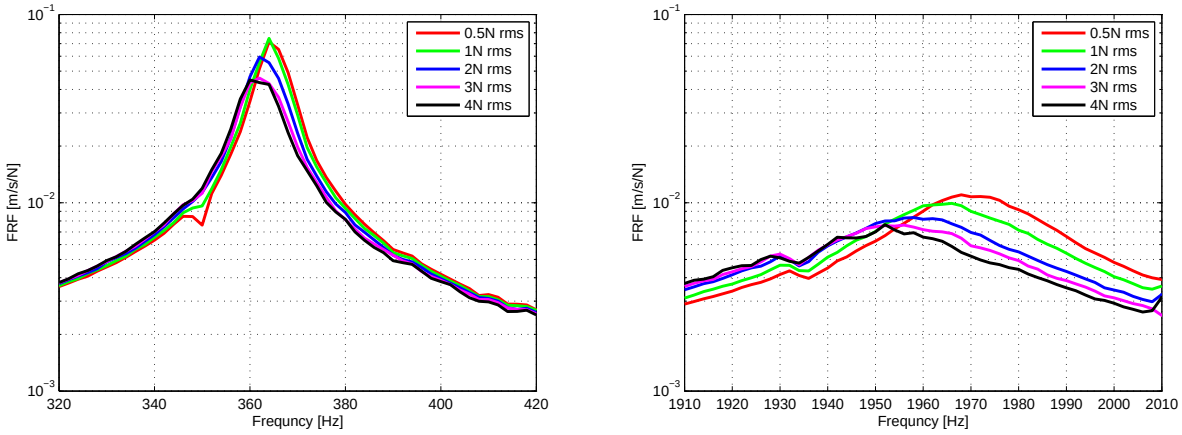

Figure 9: Variation of excitation amplitude at one end of double layered beam with bolted joints for 3Nm bolt pretension on mode 1 (left) and mode 4 (right) of vibration

From above discussion, it is evident that the proposed PDJ model can capture good convergence with experiments which are not so highly non-linear in nature. But the results were obtained with respect to a constant excitation amplitude. As it is known for the fact and discussed in the introduction section, that the excitation amplitude too has an influence onto the eigenfrequency and damping of the assembled structure. The next set of experiments will emphasize on the influence of the excitation amplitude. The shaker stinger experiment is performed on the base model, where a force transducer/sensor is attached to one end of the base model and velocity measurement with LASER vibrometer

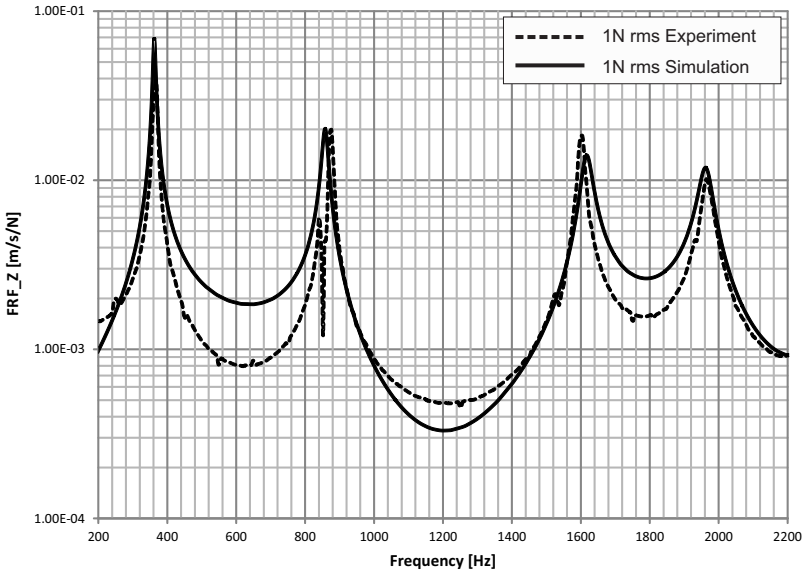

Figure 10: FRF Comparison between experiment and simulation of base model with 3Nm bolt twisting moment excited with 1N rms PSD amplitude

is done at the other end of the base model. A diagram of set-up is shown in figure 8. The bolt twisting moment of 3Nm is used considering its moderately non-linear behaviour. A random force PSD input is given from an electrodynamic Shaker and the response of the base model is observed for a set of variation in the excitation rms amplitude, as shown in figure 9.

With an increase in the excitation amplitude, the eigenfrequency decreases and the FRF mobility shape is broadened, suggesting increase in the damping. These observations are identical to the results in Geisler (2010)[17]. Increase in the excitation amplitude increases the relative motion in turn weakens the bonding pressure. Also, the effect of excitation amplitude is predominant in the higher frequency range. In simulation model, an equivalent mass of force sensor and coupling unit is attached at the excitation point of the beam. A random PSD input in frequency range from 100-3100 Hz with an equivalent bolt load of 3Nm is applied with PDJ elements at contact interface. The figure 10 shows the comparison of FRF mobility between simulation and experiment. A very good convergence between the experiment and simulation around the regions of resonances on the FRF mobility curves is obtained.

5 Conclusion

Experiment have showed that the predominant modes getting affected due to contacts are the out of plane and torsion modes. For base model testing with bolt twisting moment of 1Nm, 3Nm and 5Nm showed non-linear behaviour, slightly non-linear and linear behaviour respectively. The described discrete non-homogeneous contact model has shown very good match with experiment results of the base model. The deviation in the match for the

eigenfrequency and modal damping increases with increase in non-linearity i.e. through loosening the bolt twisting moment. Hence, can be concluded that the present model can accurately describe the systems with moderately non-linear system better than highly non-linear system. The comparison with white noise random excitation has shown a good match between simulation and experiment for a moderately non-linear system. However, these results are initial results with good match for variation in contact pressure based on the bolt twisting moment but for case of effect of large changes in excitation amplitude or complex PSD profiles, the model needs to be still quantitatively studied.

REFERENCES

[1] R. D. Mindlin, Compliance of Elastic Bodies in Contact, *Journal of Applied Mechanics* Vol. **16** 259–268, 1949.

[2] J. A. Greenwood and J. B. P. Williamson. Contact of nominally flat surfaces. *Proceedings of The Royal Society*, Vol. **295**, 300–319, 1966.

[3] H. H. Gould and B. B. Mikic, Areas of contact and pressure distribution in bolted joints, *Transactions of ASME, Jounal of Engineering for industry* 864–870, 1972.

[4] H.H. Ziad and A. K. Abd, Load pressure distribution and contact areas in bolted joints, *Institutes for Engineers (India)* Vol. **61** 93–100, 1980.

[5] C. F. Beards, *Strcutural Vibration: Analysis and Damping*. Cambridge University Press, Cambridge, 1985.

[6] M. Groper. Microslip and macroslip in bolted joints. *Experiment Mechanics*, Vol. **25**, 171–174, 1985.

[7] L. Gaul and S. Bohlen. Identification of nonlinear structural joint model and implmentation in discretized structure models. *Proc.11th ASME Conference on mechanical Vibration and Noise: The Role od Damping in Vibration and Noise, Boston (USA)*, Vol. **5**, 213–219, 1987.

[8] K. L. Johnson, *Contact Mechanics*. Arnold, Paris, 1996.

[9] B. K. Nanda and A. K. Behera. Study on damping in layered and jointed structures with uniform pressure distribution at the interfaces . *Journal of Sound and Vibration*, Vol. **226(4)**, 607–624, 1999.

[10] L. Gaul and J. Lenz. Nonlinear dynamics of structures assembled by bolted joints. *Applied mechanics Review*, Vol. **54**, 93–106, 2001.

[11] K. Worden and G. R. Tomlinson. Nonlinearity in Experimental Modal Analysis . *Phil.Trans Royal Society of London*, Vol. **359**, 113–130, 2001.

[12] K. Willner. Elasto-plastic normal contact of the three dimensional fractal surface using half space theory . *Journal of Tribology*, Vol. **126(1)**, 28–33, 2004.

[13] W. Chen and X. Deng. Structural damping caused by micro-slip along frictional interfaces . *International Journal of Mechanical Sciences*, Vol. **47**, 1191–1211, 2005.

[14] L. Gaul and M. Mayer. Modelling of Contact Interfaces in Built-up Structures by Zero-thickness Elements.

[15] M. Mayer,. *Zum Einfluss von Fuegestellen auf das dynamische Verhalten zusammengesetzter Strukturen*. Ph.D Thesis, Universitaet Stuttgart, Germany, 2007.

[16] O. Damisa et al. Dynamic Analysis of slip damping in clamped layered beams with non uniform pressure distribution at the interface . *Journal of Sound and Vibration*, Vol. **309**, 349–374, 2008.

[17] J. Gleisler,. *Numerische und experimentelle Unterschung zun dynamischen Verhalten von Strukturen mit Fuegestellen*. Ph.D Thesis, Universitt Erlangen-nrnberg, 2009.

[18] Valentin L. Popov, *Contact Mechanics and Friction*. Springer, 2010.

[19] M. Mantelli et al. Statistical model for pressure distribution of a bolted joint. *Journal of Thermophysics and Heat Transfer*, Vol. **24(2)**, 432–437, 2010.

[20] N. Peyret et.al. Energy dissipation by micro-slip in an assembly, analytic and experimental approach . *Proceedings of ASME International design Engineering technical Conference & computers and Information in engineering conference*, 2011.

[21] U. Bittner,. *Strukturakustische Optimierung von Axialkolbeneinheiten*. Ph.D Thesis, Karlsrue Institute of Technology, Germany, 2013.